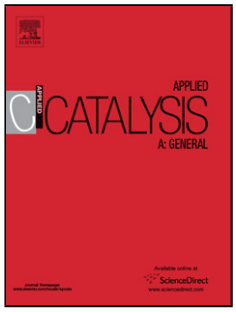

Title: Effect of annealing and nanostructuring on pulsed laser deposited WS_2 for HER catalysis

Author: Matteo Schenato Cristy Leonor Azanza Ricardo Paolo Scardi Raju Edla Antonio Miotello Michele Orlandi Rachel Morrish

PII: S0926-860X(15)30238-6
DOI: http://dx.doi.org/doi:10.1016/j.apcata.2015.11.009
Reference: APCATA 15636

To appear in: *Applied Catalysis A: General*

Received date: 3-8-2015
Revised date: 2-11-2015
Accepted date: 6-11-2015

Please cite this article as: Matteo Schenato, Cristy Leonor Azanza Ricardo, Paolo Scardi, Raju Edla, Antonio Miotello, Michele Orlandi, Rachel Morrish, Effect of annealing and nanostructuring on pulsed laser deposited WS2 for HER catalysis, Applied Catalysis A, General http://dx.doi.org/10.1016/j.apcata.2015.11.009

Effect of annealing and nanostructuring on pulsed laser deposited WS_2 for HER catalysis

Matteo Schenato[a] paolo.scardi@ing.unitn.it, Cristy Leonor Azanza Ricardo[a] antonio.miotello@unitn.it, Paolo Scardi[a], Raju Edla[b], Antonio Miotello[b], Michele Orlandi[b*] michele.orlandi@unitn.it, Rachel Morrish[c*] rmorrish@mines.edu

[a]Department of Civil, Environmental and Mechanical Engineering, University of Trento, 38123 Trento, Italy

[b]Department of Physics, University of Trento, 38123 Trento, Italy

[c]Department of Chemical and Biological Engineering, Colorado School of Mines, Golden, CO, USA 80401

[*]Corresponding author at: University of Trento(Michele Orlandi); Colorado School of Mines(Rachel Morrish).

Graphical abstract

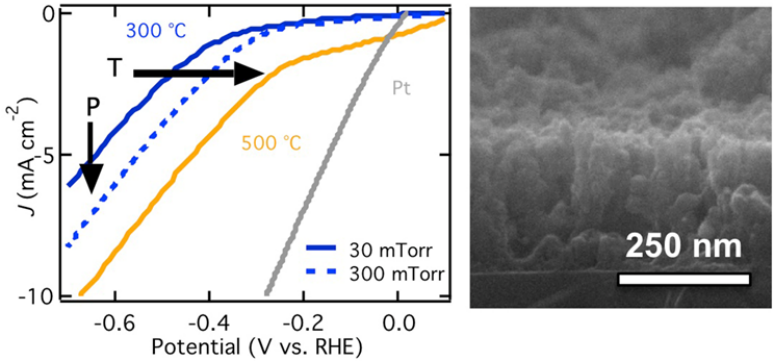

Highlights

1. Pulsed laser deposited WS_2 is found to be catalytically active toward the hydrogen evolution reaction.
2. Increasing crystallinity and introducing nanostructuring both improve electrocatalytic activity of the WS_2.
3. PLD WS_2 is a promising inexpensive, large-area, and sustainable replacement for platinum electrocatalysts.

Abstract
Replacement of platinum with cheap and abundant materials is a key step to enable the large scale application of water splitting schemes to produce hydrogen. Tungsten disulfide, a metal dichalcogenide showing catalytic activity toward the hydrogen evolution reaction (HER), is rapidly emerging as a cost effective alternative. In this paper we report the synthesis of WS_2 thin films with pulsed laser deposition (PLD), a versatile technique which combined with thermal treatments allows us to investigate the correlation between key material properties, such as crystallinity and morphology, with HER catalysis performance. Following FESEM, XRD, Raman and electrochemical characterization, we link increased activity with higher crystallinity, different from recently reported results for related materials such as MoS_2. An annealing temperature of 500 °C yields a markedly low onset potential of 160 mV relative to Pt metal and the introduction of nanostructuring proves a successful strategy for current density enhancement.

Keywords: Tungsten disulfide; Electrocatalyst; Pulsed laser deposition; Hydrogen evolution reaction

1 Introduction:

Replacement of rare and expensive platinum group catalysts is driving the search for new earth abundant materials that will help advance the hydrogen economy. Metal dichalcogenides, such as WS_2, are emerging as promising, cost effective electrocatalysts for the hydrogen evolution reaction (HER).[1] Tungsten disulfide consists of covalently bonded 2-dimensional W-S-W sheets that are held together by van der Waals forces. The edges of these semi-conducting sheets are highly active toward electrochemical water reduction while the strong covalent bonding between tungsten and sulfur imparts good material stability in aqueous solution.

Although most reports of WS_2 electrocatalysis come from single sheet morphologies,[2-4]thin films have also exhibited catalytic activity with the added benefit of large area coverage and scalable fabrication techniques.[5, 6] Pulsed laser deposition (PLD) is a versatile physical deposition method that relies on laser ablation of a target material to provide uniform coverage ranging from a few nanometers upto microns in thickness. Tungsten disulfide has previously been deposited by PLD for photonic[7] and wear applications,[8] but these films have not yet been tested for HER catalytic activity. One feature of PLD is that room temperature deposition can be achieved. This allows the impact of material structure to be easily investigated. While crystalline catalysts are typically stable with high conductivity, amorphous MoS_2 has shown unusually high concentrations of active sites. In some cases, it has even yielded superior performance.[1] A lingering question is whether the same behavior holds for WS_2. Deposition parameters also allow tuning of the film morphology, ranging from compact layers to nanostructured architectures such as nanoparticle-assembled coatings,[9] offering a strategy to improve catalysis performance by increasing the electrode surface area.

In this report, we investigate the impact of post-deposition anneal treatments on the material properties of PLD WS_2 with a specific emphasis on film crystallinity. We then proceed to introduce nanostructuring as a tool to enhance the catalytic performance. Electron microscopy, Raman spectroscopy, and X-ray diffraction were used to monitor the films as they were heated up to 600 °C. The prepared electrodes were evaluated electrochemically as potential catalysts for the HER. Because tungsten disulfide can also act as a photocatalyst, all electrodes were deposited on transparent conducting fluorine doped SnO_2 (FTO) substrates to facilitate future work testing light activated behavior.

2 Experimental:

Tungsten disulfide electrodes were prepared by PLD on FTO coated glass substrates (Sigma-Aldrich TEC 15). A cold-pressed powder (Sigma-Aldrich) target consisting of 87% 2H phase, 6% 3R phase, and the balance elemental W (by XRD) was used for the WS_2 source. The PLD tool contains a 248 nm KrF excimer laser and the energy density for all depositions was set to about 1J/cm^2. A detailed description of the apparatus is available elsewhere.[10]

All depositions were conducted at ambient temperature with a fixed sample to target distance of 3 cm. An inert Ar atmosphere of either 30 mTorr or 300 mTorr was maintained in the deposition chamber during the process. Accordingly, samples will be labeled as LP (low pressure) or HP (high pressure) in the following discussion. Approximately 1200 pulses of 25 ns duration yielded a WS_2 thickness of ~ 300 nm, which is ideal for material characterization. Post deposition annealing between 300 – 600 °C was completed under vacuum with a 10 °C/s ramp rate and a

hold time of 15 min. Longer heat treatments up to 60 minutes had no impact on electrode performance and times beyond 2 hours are known degrade grain boundaries.[11]

Samples were analyzed in a JEOL JSM-7001F field emission scanning electron microscope (FESEM) equipped with an Oxford INCA PenteFETx3 energy dispersive x-ray (EDAX) spectrometer. An accelerating voltage of 20 keV was sufficient to survey the entire WS_2 layer. Atomic ratios were corrected according to a WS_2 powder standard surveyed under the same conditions. Raman spectra were collected at room temperature on a Horiba LabAramis instrument using a 633 nm wavelength laser configured to provide a 1 cm^{-1} resolution. Crystalline phase data was obtained from X-ray diffraction with Co-Kα source on a PANalytical X'Pert MRD diffractometer. A grazing incidence angle of 2° was used on bare silicon substrates to minimize the background signal which otherwise overlaps with reflections from the WS_2 layer. The ICDD database was used for peak identification.

Electrochemical measurements were made with a Gamry Interface 1000 potentiostat using a three-electrode cell: WS_2 on FTO (working), Pt foil (counter) and saturated calomel (reference). The chosen electrolyte was 0.1 M H_2SO_4. Potential scans were collected at a rate of 10 mV/s. For clarity, all electrochemical data was corrected for pH and reported against the reversible hydrogen electrode (RHE). The reproducibility of the fabrication technique has been evaluated by testing the performance of three electrodes for each set of conditions. Potential values are reported with a 95% confidence interval.

3 Results and Discussion:

FESEM micrographs given in Figure 1 confirmed uniform coverage of the tungsten sulfide layer deposited at a low pressure of 30 mTorr. Plan view images (Fig. 1a) showed the WS_2 film consisted of smooth 100 – 200 nm features which are typical of pulsed laser deposition onto rough, FTO crystallites of approximately the same length scale.[12] The glass, FTO, and WS_2 layers are easily discerned in the tilted cross-sectional image (Fig. 1b). Thickness measurements of the PLD film consistently yielded 300 ± 25 nm for a set point of 1200 pulses.

A S:W atomic ratio of 1.4 ± 0.2 was estimated from quantitative EDAX surveys, which is low relative to the expected stoichiometric value of 2.0. Similar sulfur deficiencies have been reported for WS_2 deposited on to microfibers by PLD.[7] Low sulfur concentration in PLD WS_2 films may simply be a consequence of volatility differences between the two constituent elements. Sputter depositions of WS_2 will typically employ a sulfur rich WS_3 target followed by high temperature annealing in order to achieve stoichiometric layers.[13] For the application of HER catalysis, low sulfur content may not be a concern; sulfur defects and deficiencies have actually been linked to active catalytic sites in MoS_2.[14] Vacuum annealing did not impact the WS_2 morphology as FESEM images of heat treated samples were indistinguishable from as-deposited layers (supplementary information, Fig. S1).

A small number of 50 – 100 nm W metal particles were observed on the surface of the WS_2 films (Fig. 1a). The particles may have originated from the elemental tungsten in the powder target material, though their formation during deposition cannot be ruled out. Image analysis of low magnification micrographs (supplementary information, Fig. S2) indicates these particles have an area coverage of less than 0.5% and should not substantially impact surface behavior.

Raman spectroscopy was used to monitor the WS_2 layer as it was heated to 600 °C (Fig. 2). Spectra were collected from multiple regions on each sample to validate a homogeneous composition. The as-deposited sample exhibited the two primary reflections for WS_2 at 350 (E^1_{2G}) and 417 (A_{1G}) cm^{-1}along with a less intense peak at 326 cm^{-1}which has been assigned to a LA mode.[15] Tungsten disulfide spectra are notorious for containing a variety of convoluted second-order resonant features that can be correlated to changes in both thickness and feature morphology.[16, 17] In this case, however, annealing did not impact either and consequently the position, intensity ratio, and width of the two primary peaks remained unchanged during heating. The films annealed at 500 °C and 600 °C did exhibit intensity increases of ~25% and 45%, respectively, which is indicative of improved film crystallinity. The higher Raman signal of these samples exposed a fourth WS_2 peak at 296 cm^{-1} (2ZA) that was not discernible at low temperatures.[15]

While primarily composed of WS_2, Raman spectra revealed that WO_3 (263 cm^{-1}) was present in the films. The oxide signal decreased as the film was heated from 300 to 500 °C, but increased again for the 600 °C sample. It is likely this WO_3 formed following deposition, as WS_2 is known to oxidize under ambient exposure.[6, 18] The relative WO_3 intensity within a given sample did not change over a storage period of 6 months, indicating that once established, the oxide content is stable. Although the impact of annealing on WO_3 concentration was not rigorously examined, it seems vacuum annealing could be applied to improve the resistance of PLD WS_2 to surface oxidation. This could be particularly important for catalysis, where a significant amount of WO_3 can negatively impact performance.[5]

XRD analysis as a function of anneal temperature (Fig. 3) indicated that a heat treatment of 500 °C was required to crystallize the WS_2 layer; samples analyzed at lower temperatures contained no discernible diffraction peaks. The samples heated at 500 °C and 600 °C were both indexed to the 2H phase with primary peaks at 16.5 (002), 39.4 (100/101), and 70.6 (008) degrees (PDF# 08-0237). A weak reflection for α-W at 47.1 degrees was also detected (PDF# 04-0806) and likely stemmed from the small number of W nanoparticles observed on the film in FESEM images. The absence of XRD peaks for WO_3 supports the hypothesis of a solely superficial oxide layer. XRD surveys are representative of the entire 300 nm film with a low sensitivity to diffractions from surface layers. Conversely, the Raman signal was necessarily attenuated toward the top of the material given the relatively high optical absorption coefficient of WS_2.

The presence of (00*l*) surfaces in the XRD spectra confirms formation of extended hexagonal van der Waal planes in the deposited material.[19] Scherrer analysis[20] estimates the crystalline domains are 4 – 5 nm in size for both the 500 and 600 °C samples, which is consistent with previous reports of WS_2 heated to these temperatures.[11] The crystallites are a mixture of perpendicular (type I) and horizontal (type II) orientations given by the (100) and (002)/(008) reflections, respectively.[19] The relative intensity of the perpendicular orientation was higher for the sample heated to 500 °C. This type I orientation exposes more catalytic edge sites and is the desired alignment for electrocatalytic hydrogen production.

The prepared PLD WS_2 electrodes were examined as potential catalysts for the hydrogen evolution reaction. Current density-potential (*J* - *V*) sweeps as a function of anneal temperature

are given in Figure 4a. The required overpotential for hydrogen evolution steadily decreased as the samples were heated to 500 °C, but reverted to a higher voltage for the 600 °C sample. While the morphology and composition of the WS_2 layer remained constant during heat treatments, both Raman and XRD analysis showed an increase in crystallinity of the film. These results imply that unlike amorphous MoS_2, which exhibits high catalytic activity,[21] WS_2 performance becomes optimized for crystalline systems. A recent report arrived at a similar conclusion after comparing low and high temperature WS_2 synthesis routes.[5] In this case, the benefits of heating are only realized up to a temperature of 500 °C. The degraded performance of the 600 °C sample can be tied to several factors: a lower fraction of catalytically active type I crystallites, an increased superficial oxide layer, and most likely degradation of the underlying FTO layer. The conductivity of transparent FTO will begin to drop at temperatures > 550 °C.

Figure 4b plots the estimated onset potential for each sample. The onset potential is best evaluated at a specified current density for all data.[1] Because some scans for WS_2 exhibited a non-Faradaic linear current at low applied voltages, a conservative J value of -1.7 mA cm^{-2} was assigned as the onset point for the HER. At this value, the second derivative of the $J - V$ curve of the best performing 500 °C sample crossed zero, signifying the start of cathodic water reduction. The onset potential for the WS_2 electrodes dropped from 540 ± 20 mV for the as-deposited sample to a minimum of 210 ± 20 mV at 500 °C anneal temperature. Literature reported values for WS_2 range from ~ 350 mV for bulk films[6, 22] all the way down to a minimum of ~ 50 mV for single sheet material.[2, 3, 23]

A scan for platinum mesh was collected and analyzed under the same conditions and constraints as the WS_2 electrodes. In an ideal system, the onset potential for Pt should approach 0. Of course the reported value will vary according to the chosen J onset point. Series resistance losses as well as transport limitations can also inhibit H_2 evolution. Comparing the PLD WS_2 performance relative to the Pt baseline of 50 mV, shows a difference of only 160 mV for the 500 °C sample. This small difference puts the PLD WS_2 material on par with high performance 2D sheets[23, 24] and is quite notable given the synthesis approach is both inexpensive and easily scaled.

A second activity metric is the overpotential needed to yield a current density of 10 mA cm^{-2}, the required J value for cost competitive solar water splitting.[1] Leading exfoliated WS_2 materials have achieved 10 mA cm^{-2} at overpotentials as low as 200 mV[24] whereas thin film and bulk materials require substantially higher input voltages of 450 mV[1] and 700 mV[23], respectively. In these measurements, a potential of 660 ± 15 mV was needed to attain a current density of 10 mA cm^{-2} for the 500 °C sample. Even by thin film standards, the required voltage input for PLD films is high.[1] The large potential requirement can be partially attributed to efficiency losses in the electrochemical setup given that the required voltage for Pt mesh was nearly 280 mV.

Beyond catalytic performance, an important criterion for HER electrodes is stability. Figure 4c shows a chronoamperometry scan of a 300 °C annealed sample conducted at an applied voltage of -0.46 V vs. RHE. Following the expected drop in the first few seconds, the current density remained constant at ~2 mA cm^{-2} for a full hour. Samples annealed at 400 and 500 °C exhibited similar stability. It was noticed, however, that both the as-deposited and 600 °C treated samples were not as robust during electrochemical testing. In particular, voltage cycling caused the onset potential to steadily increase for these samples (supplementary information, Fig. S3). Since PLD

is a physical deposition technique, substrate adhesion can be a concern. Applying vacuum annealing would help alleviate this issue and explain the improved stability in the 300 – 500 °C window. Given that WS_2 itself is stable beyond 1000 °C, the declining performance of the 600 °C electrode is most likely related to degradation of the underlying FTO layer.

While the deposited WS_2 material exhibited favorable onset potentials, improvement of the *J* values is needed. One benefit of PLD is the inherent ability to induce nanostructure through pressure variation. This is particularly useful for HER catalysis because increased surface area can vastly enhance current density. The morphology of the WS_2 layer was modified by raising the deposition pressure an order of magnitude to 300 mTorr. Figure 5 shows plan view and cross-sectional FESEM images of the WS_2 material formed during the high pressure deposition. The films are rough, highly porous, and contain interconnected channels throughout the entire layer. These linked channels are important to ensure a continuous path for charge flow during catalysis. By contrast, the low pressure samples have features only on the surface, while the bulk of the film is compact (Fig. 1).

During the high pressure deposition, the presence of inert Ar gas in the chamber reduces the kinetic energy of the particles, limits the plume expansion, and promotes a high number of collisions between the ablated particles. This induces the formation of nanoclusters in the plasma plume, which are stabilized and slowed down by the background gas. Afterwards, the nano-sized agglomerates deposit on the substrate and create a porous columnar structure with intergranular voids between the columns. In low-pressure conditions, the plume expansion is less limited by the background gas, the cluster agglomeration is partially inhibited and the higher mobility ensures rearrangement of the particles after deposition on the substrate. The result is a more dense microstructure that presents porosity and defects mostly at the exposed surface region.[25, 26]

The impact of morphology on WS_2 catalytic performance was tested. Figure 6 shows linear voltage sweeps of the nanostructured high pressure samples heat treated at both 300 and 500 °C in comparison to the analogous low pressure samples. In the case of the 300 °C treatment, the high surface area behaved as expected increasing the current density over 30%. There was also a modest 50 mV improvement in the onset potential. However, for the previously optimized 500 °C heat treatment, nanostructuring actually impaired performance; the onset potential nearly doubled from 210 ± 15 mV up to 415 ± 10 mV. It was noticed that the HP samples contained a higher WO_3 signal than the LP samples (supplementary information, Fig. S4). This would be expected given superficial oxide growth on the high surface area material. An oxide layer could mask the advantages gained by nanostructuring and in the instance of the 500 °C sample, may have overwhelmed the WS_2 signal resulting in an apparent drop in performance.

4 Conclusion:

These results have shown that heat treatments can be applied to enhance the electrocatalytic performance of pulsed laser deposited WS_2 thin films. FESEM, Raman, and XRD analysis linked the increased activity to improved crystallinity rather than morphology or composition changes, which were not observed during heating. The optimized film annealed at 500 °C exhibited a low onset potential relative to platinum and was stable under both applied potential and cyclic voltammetry tests. Nanostructuring was successfully applied and it proved beneficial for HER

catalysis in the case of the 300 °C films. To fully take advantage of the nanostructuring strategy, further experiments will be needed to address the problem of superficial oxide growth.

Acknowledgement: The research activity is partially supported by the PAT (Provincia Autonoma di Trento) project ENAM in cooperation with Istituto PCB of CNR (Italy). R.M. is grateful to the U.S.-Italy Fulbright Commission for funding. The authors also acknowledge Dr. Nicola Bazzanella at the University of Trento for FESEM measurements.

Appendix A Supplementary data: Supplementary data associated with this article can be found in the online version.

References

[1] J.D. Benck, T.R. Hellstern, J. Kibsgaard, P. Chakthranont, T.F. Jaramillo, Catalyzing the Hydrogen Evolution Reaction (HER) with Molybdenum Sulfide Nanonnaterials, ACS Catalysis, 4 (2014) 3957-3971.
[2] D. Voiry, H. Yamaguchi, J.W. Li, R. Silva, D.C.B. Alves, T. Fujita, M.W. Chen, T. Asefa, V.B. Shenoy, G. Eda, M. Chhowalla, Enhanced catalytic activity in strained chemically exfoliated WS_2 nanosheets for hydrogen evolution, Nat. Mater., 12 (2013) 850-855.
[3] Z. Wu, B. Fang, A. Bonakdarpour, A. Sun, D.P. Wilkinson, D. Wang, WS_2 nanosheets as a highly efficient electrocatalyst for hydrogen evolution reaction, Appl. Catal., B, 125 (2012) 59-66.
[4] J. Kim, S. Byun, A.J. Smith, J. Yu, J. Huang, Enhanced Electrocatalytic Properties of Transition-Metal Dichalcogenides Sheets by Spontaneous Gold Nanoparticle Decoration, J. Phys. Chem. Lett., 4 (2013) 1227-1232.
[5] T.-Y. Chen, Y.-H. Chang, C.-L. Hsu, K.-H. Wei, C.-Y. Chiang, L.-J. Li, Comparative study on MoS_2 and WS_2 for electrocatalytic water splitting, Int. J. Hydrogen Energy, 38 (2013) 12302-12309.
[6] R. Morrish, T. Haak, C.A. Wolden, Low-Temperature Synthesis of n-Type WS_2 Thin Films via H_2S Plasma Sulfurization of WO_3, Chem. Mater., 26 (2014) 3986-3992.
[7] P. Yan, A. Liu, Y. Chen, H. Chen, S. Ruan, C. Guo, S. Chen, I.L. Li, H. Yang, J. Hu, G. Cao, Microfiber-based WS_2-film saturable absorber for ultra-fast photonics, Opt. Mater. Express, 5 (2015) 479-489.
[8] J.S. Zabinski, M.S. Donley, S.V. Prasad, Synthesis and characterization of tungsten disulfide films grown by pulsed-laser deposition, J. Mater. Sci., 29 (1994) 4834-4839.
[9] M. Orlandi, S. Caramori, F. Ronconi, C.A. Bignozzi, Z. El Koura, N. Bazzanella, L. Meda, A. Miotello, Pulsed-Laser Deposition of Nanostructured Iron Oxide Catalysts for Efficient Water Oxidation, ACS Appl. Mater. Interfaces, 6 (2014) 6186-6190.
[10] M. Bonelli, C. Cestari, A. Miotello, Pulsed laser deposition apparatus for applied research, Meas. Sci. Technol., 10 (1999) N27 - N30.
[11] S.J. Li, J.C. Bernede, J. Pouzet, M. Jamali, WS_2 thin films prepared by solid state reaction (induced by annealing) between the constituents in thin film form, J. Phys.: Condens. Matter, 8 (1996) 2291-2304.
[12] S. Vijayalakshmy, B. Subramanian, Effect of ZnO block layers fabricated by Pulsed Laser Deposition and mesoporous layers by chemical method on the performance of dye sensitized solar cells, Electrochim. Acta, 137 (2014) 131-137.
[13] S. Brunken, R. Mientus, K. Ellmer, Metal-sulfide assisted rapid crystallization of highly (001)-textured tungsten disulphide (WS_2) films on metallic back contacts, Phys. Status Solidi A, 209 (2012) 317-322.
[14] J. Xie, J. Zhang, S. Li, F. Grote, X. Zhang, H. Zhang, R. Wang, Y. Lei, B. Pan, Y. Xie, Controllable Disorder Engineering in Oxygen-Incorporated MoS_2 Ultrathin Nanosheets for Efficient Hydrogen Evolution, J. Am. Chem. Soc., 135 (2013) 17881-17888.
[15] W. Zhao, Z. Ghorannevis, K.K. Amara, J.R. Pang, M. Toh, X. Zhang, C. Kloc, P.H. Tan, G. Eda, Lattice dynamics in mono- and few-layer sheets of WS_2 and WSe_2, Nanoscale, 5 (2013) 9677-9683.

[16] M. Krause, M. Virsek, M. Remskar, N. Salacan, N. Fleischer, L. Chen, P. Hatto, A. Kolitsch, W. Moeller, Diameter and Morphology Dependent Raman Signatures of WS_2 Nanostructures, Chemphyschem, 10 (2009) 2221-2225.
[17] C. Sourisseau, F. Cruege, M. Fouassier, M. Alba, 2nd-Order Raman Effects, Inelastic Neutron-Scattering and Lattice-Dynamics in 2H-WS_2, Chem. Phys., 150 (1991) 281-293.
[18] S.B. Sadale, P.S. Patil, Synthesis of type-I textured tungsten disulfide thin films on quartz substrate, J. Cryst. Growth, 286 (2006) 481-486.
[19] A. Ennaoui, K. Diesner, S. Fiechter, J.H. Moser, F. Levy, Structural analysis of 2H-WS_2 thin films by X-ray and TEM investigation, Thin Solid Films, 311 (1997) 146-150.
[20] H.P. Klug, L.E. Alexander, X-Ray Diffraction Procedures: For Polycrystalline and Amorphous Materials, Wiley-Interscience1974.
[21] D. Merki, S. Fierro, H. Vrubel, X. Hu, Amorphous molybdenum sulfide films as catalysts for electrochemical hydrogen production in water, Chem. Sci., 2 (2011) 1262-1267.
[22] J. Yang, D. Voiry, S.J. Ahn, D. Kang, A.Y. Kim, M. Chhowalla, H.S. Shin, Two-Dimensional Hybrid Nanosheets of Tungsten Disulfide and Reduced Graphene Oxide as Catalysts for Enhanced Hydrogen Evolution, Angew. Chem. Int. Edit., 52 (2013) 13751-13754.
[23] J. Yang, H.S. Shin, Recent advances in layered transition metal dichalcogenides for hydrogen evolution reaction, J. Mater. Chem. A, 2 (2014) 5979-5985.
[24] C.G. Morales-Guio, L.-A. Stern, X. Hu, Nanostructured hydrotreating catalysts for electrochemical hydrogen evolution, Chem. Soc. Rev., 43 (2014) 6555-6569.
[25] A. Infortuna, A.S. Harvey, L.J. Gauckler, Microstructures of CGO and YSZ thin films by pulsed laser deposition, Adv. Funct. Mater., 18 (2008) 127 - 135.
[26] I. Petrov, P.B. Barna, L. Hultman, J.E. Greene, Microstructural evolution during film growth, J. Vac. Sci. Technol., A, 21 (2003) S117 - S128.

Figure Captions

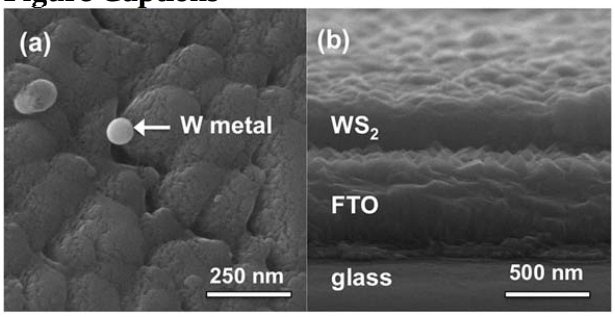

Figure 1: FESEM images of LP PLD WS_2 (a) plan view and (b) tilted cross-section.

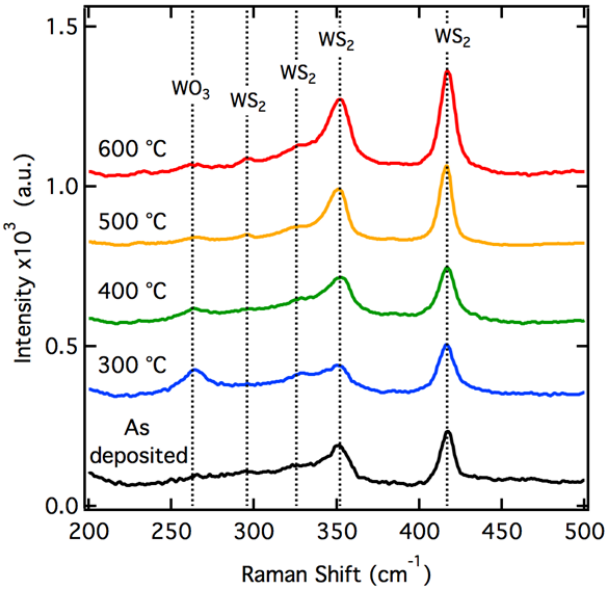

Figure 2: Raman spectra of LP PLD WS_2 as a function of anneal temperature.

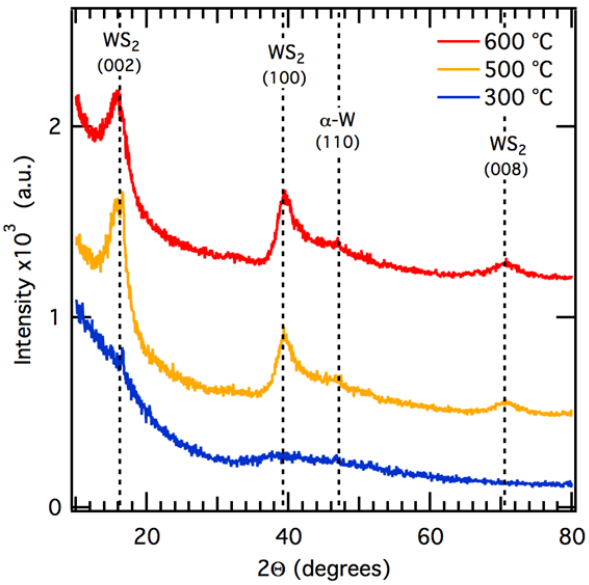

Figure 3: Grazing incidence XRD spectra of LP PLD WS_2 at 300, 500, and 600 °C.

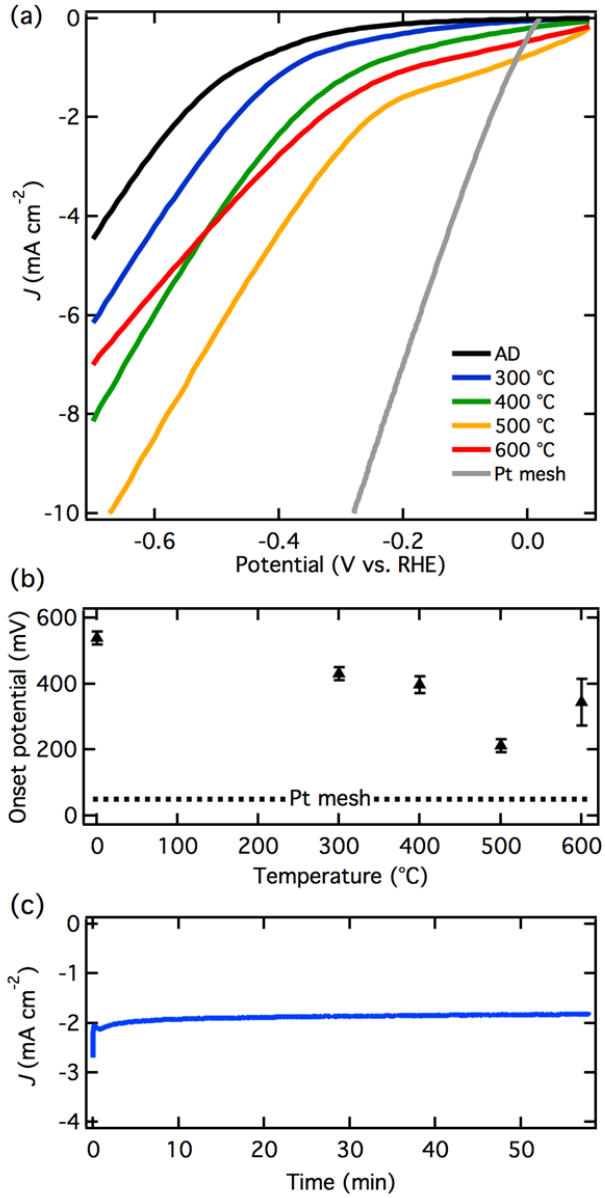

Figure 4: (a) J –V behavior of LP PLD WS_2 electrodes as a function of temperature in 0.1 M H_2SO_4 (b) onset potential as a function of temperature evaluated at -1.7 mA cm^{-2}; the error bars represent 95% confidence intervals for three replicate measurements (c) chronoamperometry plot of a 300 °C WS_2 electrode (V = -0.46 vs. RHE).

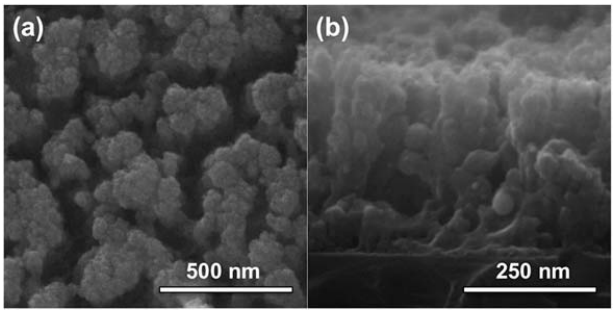

Figure 5: FESEM images of HP PLD WS_2 (a) plan view and (b) cross-section.

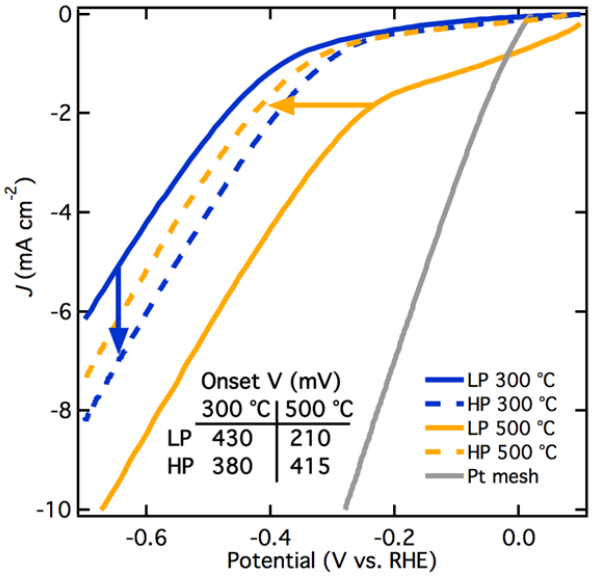

Figure 6: *J* –*V* behavior of the low pressure (LP) and high pressure (HP) PLD WS_2 electrodes in 0.1 M H_2SO_4. Tabulated values of the onset potential are also shown.